Cell Stem Cell
Article

Extensive Hematopoietic Stem Cell Generation in the AGM Region via Maturation of VE-Cadherin^{+}CD45^{+} Pre-Definitive HSCs

Samir Taoudi,[1] Christèle Gonneau,[1] Kate Moore,[1] Julie M. Sheridan,[1] C. Clare Blackburn,[1] Erin Taylor,[1] and Alexander Medvinsky[1,*]
[1]MRC Centre for Regenerative Medicine, Institute for Stem Cell Research, University of Edinburgh, Edinburgh EH9 3JQ, UK
*Correspondence: a.medvinsky@ed.ac.uk
DOI 10.1016/j.stem.2008.06.004

SUMMARY

Elucidating the mechanisms underlying hematopoietic stem cell (HSC) specification and expansion in the embryo has been hampered by the lack of analytical cell culture systems that recapitulate in vivo development. Here, we describe an ex vivo model that facilitates a rapid and robust emergence of multipotent long-term repopulating HSCs in the embryonic AGM region. Because this method includes a cell dissociation step prior to reconstruction of a three-dimensional functional tissue and preserves both stromal and hematopoietic elements, it allowed us to identify the direct ancestry of the rapidly expanding HSC pool. We demonstrate that extensive generation of definitive HSCs in the AGM occurs predominantly through the acquisition of stem characteristics by the VE-cadherin^{+}CD45^{+} population.

INTRODUCTION

Hematopoietic stem cell (HSC) development during ontogeny is a complex developmental cascade, the mechanisms of which remain poorly understood. Prior to fetal liver colonization, HSCs emerge in multiple extrahepatic locations between embryonic days (E) 10.5–11.5 (Gekas et al., 2005; Kumaravelu et al., 2002; Medvinsky and Dzierzak, 1996; Morrison et al., 1995; Ottersbach and Dzierzak, 2005). Between E11.5 and E12.5, HSCs are generated at an extremely high rate: from three to ten HSCs in the entire E11.5 conceptus to 70 to 150 HSCs by E12.5 (Gekas et al., 2005; Kumaravelu et al., 2002). The mechanism by which this massive expansion occurs can be explained either by the rapid proliferation of pre-existing HSCs or by the maturation of HSCs from as yet unknown ancestor cells (Dzierzak and Medvinsky, 1995; Ferkowicz et al., 2003). Neither transgenic approaches nor culture techniques described to date have provided a methodology to discriminate between these alternatives.

The explant culture system has successfully been used in developmental biology as a tool for dissecting mechanisms of morphogenesis and differentiation of various organ rudiments (Moscona and Moscona, 1952b; Shannon and Hyatt, 2004). Based on this principle, ex vivo culture methods have been designed to study the spatial origins of HSC development in the embryo (Cumano et al., 2001; de Bruijn et al., 2000; Kumaravelu et al., 2002; Medvinsky and Dzierzak, 1996; Taoudi and Medvinsky, 2007). It has been demonstrated that, between E10.5 and E11.5, the AGM region is capable of an autonomous initiation and expansion of bona fide definitive HSCs (Medvinsky and Dzierzak, 1996); this can be enhanced by the addition of exogenous interleukin-3 (Robin et al., 2006). However, the accessibility of AGM explants for mechanistic analysis is highly restricted. Therefore, attempts to elucidate developmental cues that underlie HSC specification and expansion have focused on the derivation and use of stromal cell lines. Although these cell lines were able to maintain adult bone marrow HSCs (Ohneda et al., 1998; Oostendorp et al., 2002; Xu et al., 1998), they have not yielded any greater mechanistic insight into the process of HSC generation.

Classical embryological studies have demonstrated that a number of dissociated embryonic organs are capable of both reorganization and continuation along their specified developmental pathways upon reaggregation. Using this approach, fundamental biological processes within complex organs have been elucidated (Anderson et al., 1993; Grobstein, 1953; Moscona and Moscona, 1952a; Townes and Holtfreter, 1955; White et al., 2007). Based on the principle of organ reaggregation, we developed a robust analytical culture system that facilitates an unprecedented HSC expansion at a level comparable to that observed in vivo. Crucially, this system allows controlled manipulation of defined AGM cell populations prior to continued ex vivo development. Herein, we demonstrate that the VE-cadherin^{+}CD45^{+} fraction of the E11.5 AGM region, which is spatially restricted to intra-aortic clusters, contains pre-HSCs capable of rapidly maturing into functional definitive HSCs.

RESULTS

Successful Ex Vivo HSC Maintenance following Dissociation and Reaggregation of the E11.5 AGM Region

Previously, attempts to preserve definitive HSC activity in vitro from a single-cell suspension of E11.5 AGM have been unsuccessful (data not shown). This deficiency has hampered progress into dissecting the mechanisms of HSC specification and expansion in primary embryonic hematopoietic organs. To overcome this obstacle, we made two crucial developments. The first was to define a medium that could facilitate HSC expansion. The

second was to develop a technique that would both enable the preservation of HSC activity in the AGM region following disaggregation of the organ's original structure and allow a period of ex vivo development to be undertaken.

Using IMDM-based medium supplemented with interleukin-3 (IL3), stem cell factor (SCF), and Flt3-ligand (Flt3L) (referred to as IMDM$^+$ medium), we were able to preserve the ex vivo capacity of the E11.5 AGM region to generate HSCs after dissociation and reaggregation of the organ (Figure S1 of Supplemental Data available online). Of note, successful maintenance of stromal elements (including endothelial cells) and HSCs required culture of dissociated tissues at the gas-liquid interface (Figure S1). HSCs within the AGM reaggregate were capable of long-term multilineage reconstitution (Figure S2) and contributed to the recipient HSC compartment, as evidenced by successful secondary transplantations (Figure S3).

During ex vivo development of the reaggregated AGM region, the hematopoietic (CD45-expressing) compartment underwent extensive expansion, increasing from 3,640 ± 310 to 32,130 ± 5,960 cells within a 96 hr period (Figures 1A and S4). Functional examination revealed that a massive expansion of committed myeloid progenitors (colony-forming units-culture [CFU-C]) and immature late-developing colony-forming units-spleen (CFU-S_{11}) had also occurred. Specifically, CFU-Cs expanded 45-fold (120 ± 15 to 5,440 ± 120) (Figure 1B), and CFU-S_{11} expanded 230-fold (3.3 ± 2.0 to 770 ± 390) (Figure 1C).

Quantification of HSC Generation

To assess expansion of the HSC compartment, the total numbers of HSCs produced in the system were determined in a series of in vivo transplantation experiments. In line with previous data (Gekas et al., 2005; Kumaravelu et al., 2002), no more than one HSC was detected per single uncultured E11.5 AGM region (one out of four experimental mice were repopulated; Figure 1D). We then carried out time course experiments to characterize the temporal kinetics of HSC formation. Between 24 and 48 hr, no HSC expansion had occurred, since no more than one HSC per single reaggregate dose was detected (Figure 1D). However, at 72 and 96 hr of culture, each mouse that received a transplant of 0.5 dose of reaggregate was repopulated at a high level (Figure 1D), indicating that HSC expansion occurs in the final 48 hr of culture.

To accurately calculate the absolute number of HSCs present at 72 and 96 hr of culture in vivo, limiting dilution studies were performed. These data demonstrated that approximately six HSCs per reaggregate were present at 72 hr (Figure 1E) and approximately 150 HSCs per reaggregate at 96 hr (Figure 1F). Thus, unlike the progenitor compartment that undergoes linear expansion, the HSC compartment expands exponentially between 72 and 96 hr of culture, indicating the occurrence of either a very rapid proliferation of the single pre-existing HSC or a mass maturation of HSC ancestors (pre-HSCs). Notably, the presence of all three growth factors (IL3, SCF, and Flt3L) was required to facilitate a 150-fold expansion of HSCs (Figure S5).

Acquisition of Stem Cell Function Is the Predominant Mechanism of HSC Generation

Consistent with the observed extensive and rapid production of hematopoietic cells within AGM reaggregates, we found that, in comparison with other lineages, a greater proportion of CD45$^+$ cells were in S phase of cell cycle (Figure S6). These data indicated that rapid proliferation might be a key mechanism for HSC expansion. Thus, to establish the proliferative history of stem and progenitor cells, a cellular suspension of E11.5 AGM was loaded with the dye carboxyfluoroscein diacetate succinimidyl ester (CFSE). As previously described (Lyons, 1999), CFSE is distributed between daughter cells at division such that fluorescence intensity diminishes by half at each mitosis, allowing the number of divisions to be determined by flow cytometry. At the 96 hr endpoint, the cells present within the reaggregate demonstrated a differential retention of CFSE, reflecting differences in proliferative history during the culture (Figure 2A). Consistent with the majority of CD45$^+$ cells being in S phase, most hematopoietic cells retained low to undetectable levels of CFSE.

We then identified the following CD45$^+$ fractions on the basis of proliferative history: high proliferating (fraction A, approximately five to seven divisions), low proliferating (fraction B, approximately one to four divisions), and nondividing (fraction C, zero divisions) (Figure 2A). Gating of fraction C was based on the analysis of reaggregates cultured in the presence of the mitotic inhibitor demecolcine, which provided a control for the level of CFSE expected within nondividing cells (data not shown). All nonhematopoietic (CD45$^-$) lineages were grouped as fraction D.

Fractions A–D were purified by flow cytometry and studied morphologically and functionally (Figure 2A). Fraction A contained a high frequency of cells with classical blast (stem/progenitor) cell morphology characterized by a high nuclear-to-cytoplasmic ratio (Figure 2A). Fraction B also contained blast-like cells, but a higher frequency of differentiated cells was also observed. All nonproliferating cells purified from fraction C appeared to have a fully differentiated morphology (Figure 2A). Cell cycle analysis of fractions A–C after 96 hr demonstrated that the majority of cells in fraction A were within the active phases of the cell cycle (Figure 2A). In contrast, the vast majority of cells in fractions B and C were in the G_0/G_1 position of the cycle.

Fractions A, B, and C were tested functionally for the contents of CFU-Cs, upstream immature myeloid CFU-S_{11}, and definitive HSCs. While nearly all CFU-Cs resided in the highly proliferative fraction A (Figure 2B), most CFU-S_{11} and HSCs were contained within the slowly dividing fraction B (Figures 2C and 2D); only 4 out of 11 recipients were repopulated after receiving a 0.05 dose of fraction A, while all 11 recipients of fraction B were successfully repopulated (Figure 2D). We estimate that there are approximately eight HSCs in fraction A with the remaining 140 HSCs residing in fraction B. Thus, the vast majority of HSCs underwent a limited number of divisions.

Although CFU-S and HSC compartments underwent the greatest fold increase, 230- and 150-fold, respectively, they underwent fewer divisions than CFU-Cs (Figures 2B–2D). The fact that the HSCs underwent no more than four divisions is not compatible with the idea that they originate from a single parental HSC. For this to have occurred, a minimum of seven to eight symmetrical divisions would be required, which would result in undetectable levels of CFSE. Thus, HSC generation occurs predominantly via an acquisition of stem cell characteristics by HSC ancestors (pre-HSCs) rather than by rapid amplification of a pre-existing single HSC.

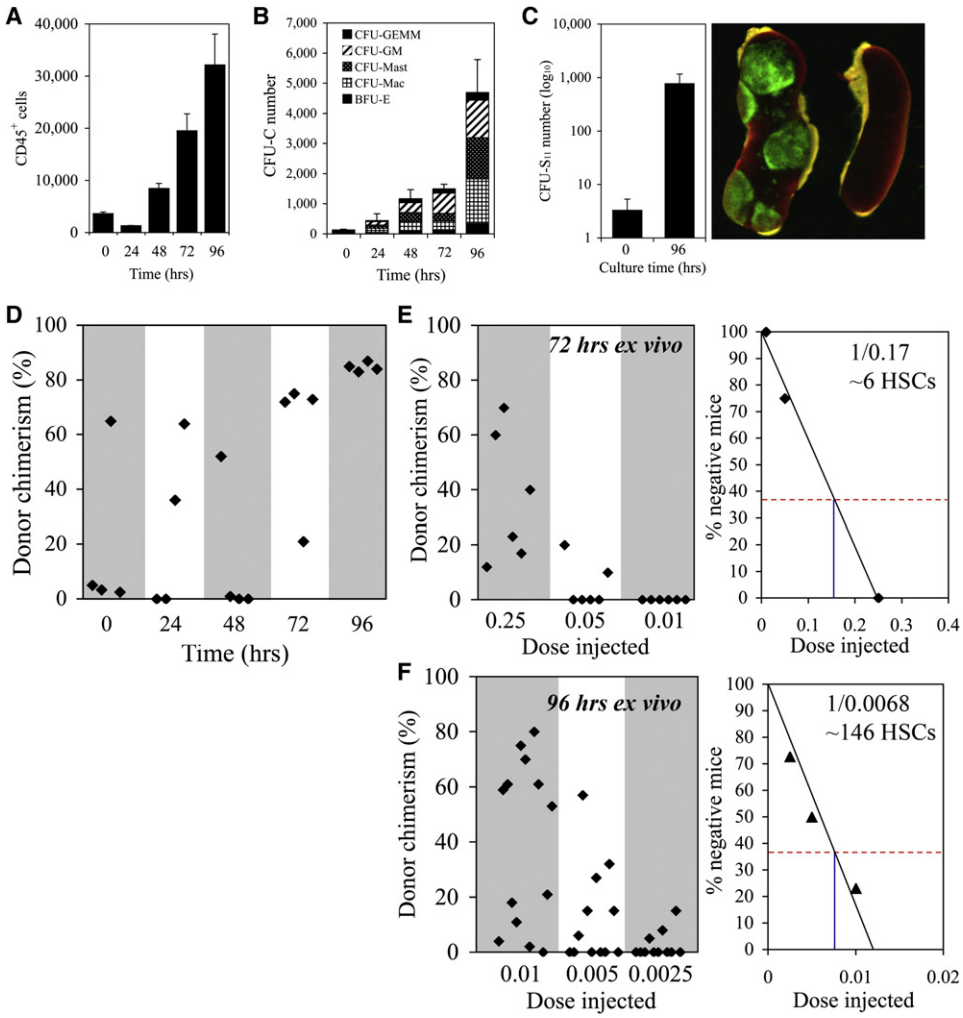

Figure 1. Rapid Ex Vivo HSC Generation in the AGM Region

(A and B) The hematopoietic ($CD45^+$) compartment undergoes extensive expansion during culture, as do all types of CFU-C. Data indicate the numbers of total $CD45^+$ cells and CFU-Cs per reaggregate (three independent experiments ± SEM).

(C) Expansion of late-developing colony-forming unit-spleen ($CFU\text{-}S_{11}$) after 96 hr (three independent experiments ± SD). The donor origin of spleen colonies was confirmed using reaggregates produced from $EGFP^+$ embryos (left spleen); no colonies were detected in irradiated control mice (right spleen).

(D) Time course of HSC generation during ex vivo development. At 24, 48, 72, and 96 hr, cells were transplanted; each recipient received a 0.5 dose of reaggregate. Each point represents an individual recipient mouse. Data are cumulative of two independent experiments.

(E and F) Statistical analysis of limiting dilution experiments indicates the presence of approximately six HSCs and 146 HSCs per reaggregate after 72 hr and 96 hr, respectively.

To investigate the spatial aspect of HSC development within the AGM reaggregate, we first identified the immunophenotype of the stem cell compartment. To this end, cell fractions generated within the reaggregate after 96 hr were sorted by flow cytometry on the basis of known stem cell markers and tested in long-term repopulation experiments. We found that the AGM-derived HSC population had adopted an adult-like bone marrow HSC immunophenotype: $CD45^+cKit^+Sca1^+PECAM\text{-}1^{low}CD34^-$ phenotype (Figure 3A) (Baumann et al., 2004; Osawa et al., 1996; Uchida and Weissman, 1992). The lack of CD34 expression indicates that the fetal liver stage, which involves sustained CD34 expression (Matsuoka et al., 2001), had been bypassed. From our CFSE experiments, we estimate that the frequency of HSCs in fraction B ($CD45^+CFSE^{low}$) is 1 in 80 cells (140 HSCs in 11,160 total fraction B cells). When Sca1 is also included in the selecting cocktail, the enrichment for HSCs is increased to 1 in 15 cells, as only 19% ± 3.5% of fraction B cells coexpress Sca1 (Figure 3B).

This phenotypic analysis allowed us to investigate the spatial distribution of progenitor and stem cells within the reaggregate using confocal microscopy (Figure 3C). We found that CFU-C progenitors ($CD45^+CFSE^{neg}$ cells) were located in large colonies (Figures 3D and 3D′). HSCs ($CD45^+CFSE^{low}Sca1^+$) were not found within these same colonies but were located separately either in small clusters (Figures 3E and 3E′) or as individual cells (Figures 3F and 3F′). This observation is consistent with our

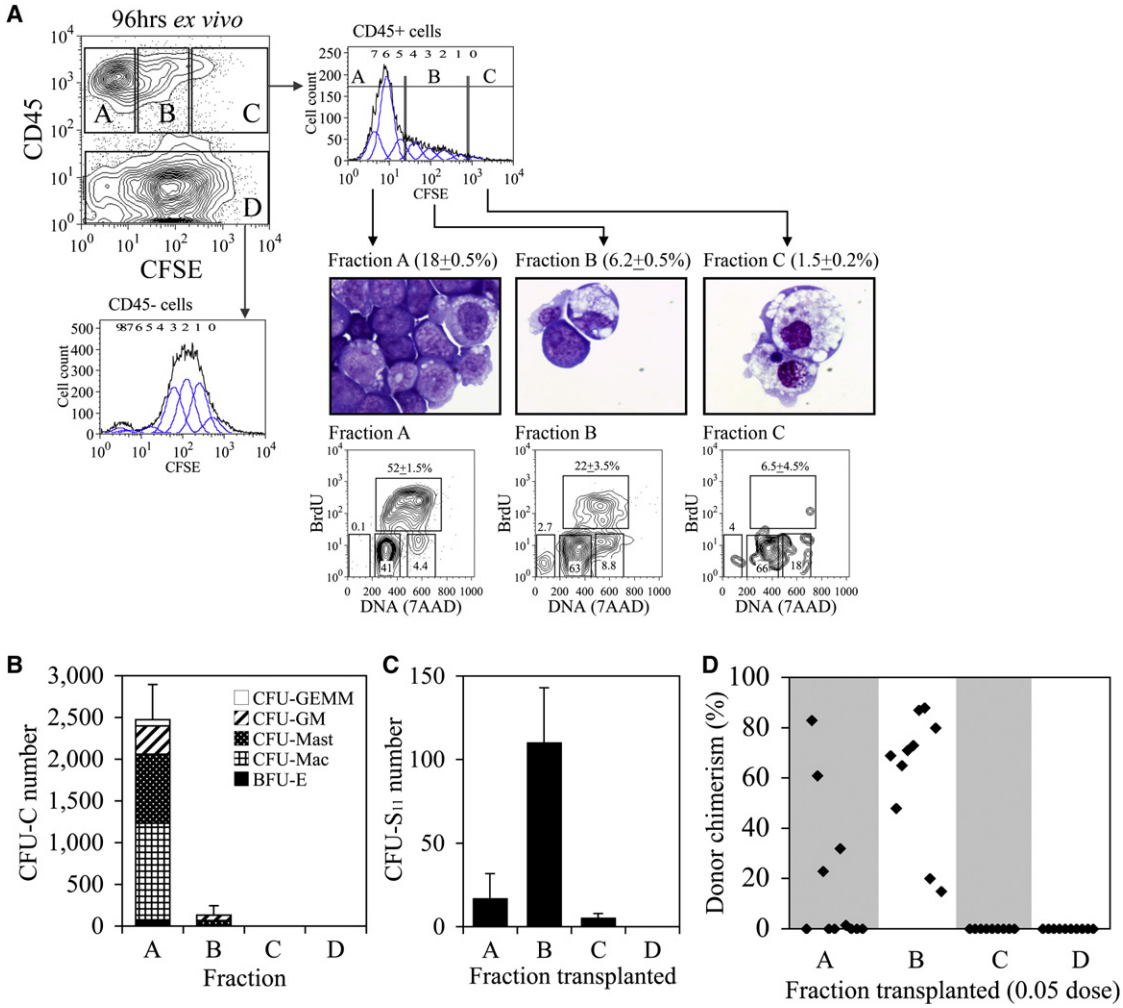

Figure 2. Tracing the HSC Proliferative History following AGM Ex Vivo Development

(A) Cell suspension from E11.5 AGM was loaded with carboxyfluoroscein diacetate succinimidyl ester (CFSE) prior to culture. After 96 hr, the expanded hematopoietic ($CD45^+$) population was segregated according to proliferative history based on CFSE loss. Fraction A ($CFSE^{neg}CD45^+$) underwent five to seven divisions; fraction B ($CFSE^{low}CD45^+$), one to four divisions; fraction C ($CFSE^{high}CD45^+$), zero divisions. The majority of nonhematopoietic lineages (fraction D) underwent approximately one to four divisions. Numbers indicate the numbers of divisions. Contour plot illustrates the placement of gates for fractions A–D; sorted fractions A–C are shown on cytospin preparations stained with May-Grunwald-Giemsa. The percentages of each fraction per reaggregate are shown (three independent experiments ± SEM). Cell cycle analysis of fractions A–C. Shown are the percentages of cells in S phase (three independent experiments ± SEM).

(B) The vast majority of colony-forming units-culture (CFU-C) are restricted to fraction A (three independent experiments ± SEM).

(C) In contrast, nearly all colony-forming units-spleen ($CFU\text{-}S_{11}$) reside in fraction B (two independent experiments ± SD).

(D) The vast majority of HSCs also reside in fraction B. Each dot represents one recipient that had received a 0.05 dose of a respective purified fraction. Data are cumulative of three independent experiments.

conclusion that the pool of HSCs matures from multiple pre-HSCs via a restricted number of divisions.

The $CD45^+$ Compartment Is the Major Contributor to HSC Expansion in the AGM Reaggregate

To determine the pre-HSCs' identities, we investigated whether hematopoietic ($CD45^+$) or nonhematopoietic ($CD45^-$) cells were capable of developing into HSCs. To this end, $CD45^+$ cells from wild-type (WT) E11.5 AGM regions were replaced by MACS-purified $CD45^+$ cells from EGFP E11.5 AGM regions (Figure 4A). Cells were mixed at the quantitative ratio observed in the E11.5 AGM region (~135,000 WT $CD45^-$ cells and 5,000 EGFP $CD45^+$ cells, i.e., to produce a reaggregate with an initial cellularity equivalent to one fresh E11.5 AGM) and chimeric reaggregates were produced. After 96 hr of culture, the vast majority (95% ± 0.9%) of hematopoietic cells in these chimeric reaggregates were derived from EGFP $CD45^+$ ancestors (Figure 4B).

We then traced the lineage ancestry of definitive HSCs by transplantation of the chimeric reaggregates into irradiated Ly5.2/1 adult mice and detecting donor-derived cells in the peripheral blood of recipient mice (Figure 4C). All nine recipient

A

Population	Reconstituted/total injected
$CD45^+$	8/8
$CD45^-$	0/11
$CD45^+CD34^+$	0/6
$CD45^+CD34^-$	7/7
$CD45^+cKit^+$	6/14
$CD45^+cKit^-$	0/16
$CD45^+cKit^{high}$	1/4
$CD45^+cKit^{low}$	4/4
$CD45^+Sca1^+$	4/10
$CD45^+Sca1^-$	0/10
$CD45^+PECAM\text{-}1^{high}$	0/5
$CD45^+PECAM\text{-}1^{low}$	3/5
$CD45^+PECAM\text{-}1^-$	0/3

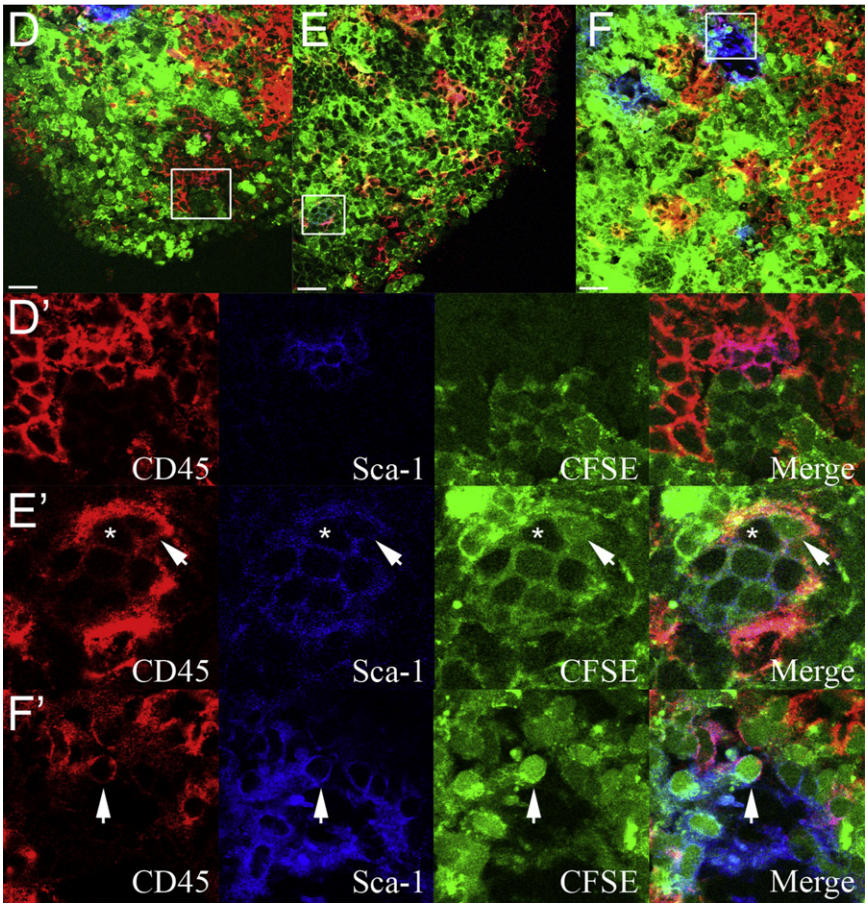

Figure 3. Spatial Compartmentalization of Stem and Progenitor Cells in the Reaggregated AGM Region

(A) The immunophenotype of HSCs produced after 96 hr was determined by transplanting defined cellular populations, purified by flow cytometry, into irradiated adult mice. Indicated is the number of reconstituted animals as a fraction of the total number of recipients. HSCs derived from the E11.5 AGM region adopt an adult-like $CD45^+cKit^+Sca1^+PECAM\text{-}1^{low}CD34^-$ immunophenotype.

(B) The vast majority of HSCs can be isolated as $CD45^+CFSE^{low}Sca1^+$ cells, enriching HSCs to approximately 1 in 15 cells.

(C) E11.5 AGMs were dissociated, loaded with CFSE (green), and reaggregated. After 96 hr ex vivo, the reaggregate was prepared for confocal microscopy. Sections were stained using anti-CD45 (red) and anti-Sca1 (blue) antibodies (scale bar, 70 μm).

(D and D′) Areas of CFU-C progenitors ($CD45^+CFSE^{neg}$) are readily identified.

(E, E′, F, and F′) $CD45^+CFSE^{low}Sca1^+$ (HSCs) are found segregated either in small clusters or as single cells dispersed within the central region of the reaggregate (scale bar, 37 μm).

(D′–F′) Zooms of boxed regions shown in (D)–(F); shown are CFSE-retaining HSCs (arrowheads) and $CFSE^-$ hematopoietic cells (asterisk). Images are representative sections from four individual reaggregates.

mice were reconstituted with $EGFP^+$ HSCs derived from the $CD45^+$ compartment. Consistent with HSCs generated by WT reaggregates (Figure S2), $EGFP^+$ cells contributed to both myeloid and lymphoid lineages in all tissues tested (data not shown). Only one recipient mouse also contained donor-derived blood cells of $CD45^-$ ancestry (Figure 4C). Although we were able to use highly purified $CD45^-$ cells, the possibility of contamination with rare but highly potent $CD45^+$ cells cannot be excluded. Thus, we conclude that the vast majority of HSCs in the AGM reaggregate were generated by the maturation of CD45-expressing pre-HSCs.

Pre-HSCs Reside within the VE-Cadherin$^+$CD45$^+$ Subfraction of the Hematopoietic Compartment

The first HSC emerging in the AGM bears a distinctive dual hemato-endothelial immunophenotype coexpressing both VE-cadherin and CD45 markers (North et al., 2002; Taoudi et al., 2005). Among 70 VE-cadherin$^+$CD45$^+$ cells contained in the E11.5 AGM region, one is a definitive HSC (Figure 1D) (Gekas et al., 2005; Kumaravelu et al., 2002; Taoudi et al., 2005). The functional capacity of other VE-cadherin$^+$CD45$^+$ cells is unclear.

While $CD45^+$ cells are scattered throughout the entire E11.5 AGM region (Figure 5A), cells of the VE-cadherin$^+$CD45$^+$ fraction are intimately associated with the endothelial lining of the dorsal aorta, represented as cuboid epithelium. They are either integrated into the endothelial lining (Figures 5B and 5B′) or they form intra-aortic clusters protruding into the aortic lumen (Figures 5C and 5C′). We observed that each E11.5 AGM region typically contains two to four of these intra-aortic clusters. Polarized localization of both CD45 and VE-cadherin

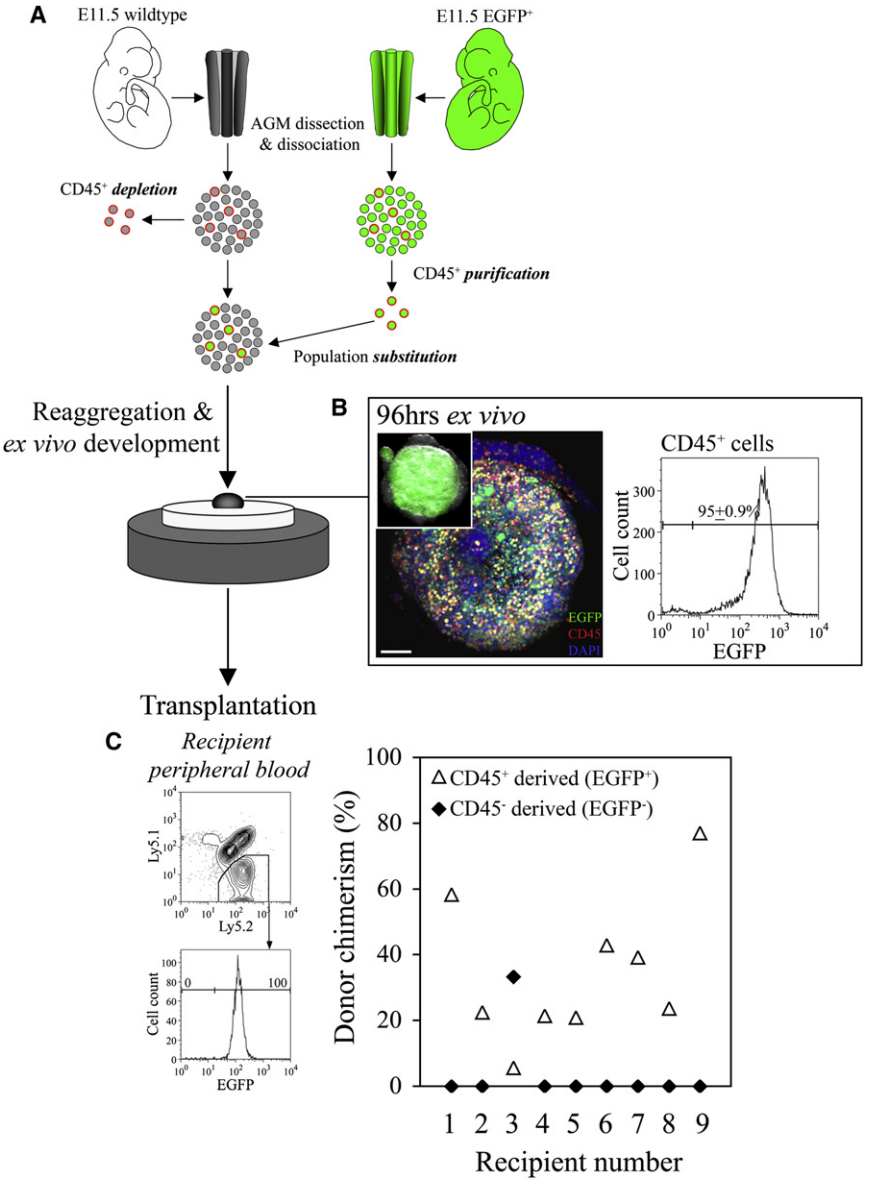

Figure 4. Tracing the Lineage Ancestry of the Generated HSC Pool

(A) Dissociated cells from the AGM can be manipulated prior to culture. The developmental potential of $CD45^+$ cells was traced by replacement of wild-type cells with an $EGFP^+$ counterpart. After ex vivo development, reaggregates were dissociated and transplanted into irradiated adult (Ly5.2/1) recipients along with bone marrow (Ly5.1/1) carrier cells.

(B) Chimeric reaggregates were constructed by mixing 135,000 wild-type $CD45^-$ cells and 5,000 $EGFP^+$ $CD45^+$ cells and allowed to develop ex vivo for 96 hr. Shown is a 3D confocal reconstruction illustrating $EGFP^+CD45^+$ cells within the chimeric reaggregate (scale bar, 75 μM). (Inset) A low-magnification EGFP fluorescence/bright-field overlay (original magnification 60×). The vast majority of the expanded ($CD45^+$) hematopoietic compartment was found to have derived from $CD45^+$ ancestry (data are representative of seven independent experiments).

(C) After 96 hr, 0.05 doses of reaggregate were transplanted into each irradiated adult recipient. Lineage ancestry of engrafting cells was resolved according to EGFP expression. HSCs derived from $CD45^+$ ancestors were detected in all recipient animals (data are cumulative of two independent experiments).

proteins in these clusters emphasizes their epithelial-like organization, consistent with the fact that they originate from the endothelial lining. In rare cases, solitary VE-cadherin$^+$CD45$^+$ cells are associated with the luminal surface of the endothelial lining (data not shown).

To investigate whether the VE-cadherin$^-$CD45$^+$ or VE-cadherin$^+$CD45$^+$ populations harbor pre-HSCs, we performed further lineage-tracing experiments. To this end, each population was purified by flow cytometry from AGM regions dissected from E11.5 EGFP embryos (Figure 6A) and reaggregated with $CD45^-$ cells purified from WT AGM regions (Figure 6B). Following 96 hr of ex vivo development, only a modest expansion of hematopoietic cells was observed from the VE-cadherin$^-$CD45$^+$ population; from ~5,000 input cells, 5,530 ± 1,550 $CD45^+$ cells were detected after culture (Figure 6C). Transplantation of a 0.05 dose of these chimeric reaggregates per recipient (after 96 hr ex vivo) revealed that no HSCs had been generated (Figure 6D). In contrast, the input population of 70 VE-cadherin$^+$CD45$^+$ cells aggregated with WT $CD45^-$ cells had undergone a 240-fold expansion resulting in formation of a pool of 16,850 ± 4,700 $CD45^+$ cells (Figure 6E). Upon transplantation of a 0.05 dose of reaggregate per recipient, all experimental mice were reconstituted at a high level (Figure 6F) and demonstrated myeloid and lymphoid contribution to all tissues analyzed (Figure S7). Therefore, pre-HSCs within the hematopoietic compartment of the E11.5 AGM region are located within the VE-cadherin$^+$CD45$^+$ population.

DISCUSSION

We have developed an ex vivo model capable of rapidly generating definitive HSCs from an embryonic organ, which recapitulates the rapid HSC expansion observed within the midgestation embryo. A short dissociation step and manipulation of cell subpopulations prior to reconstruction of the functionally active AGM organoid allowed us to obtain previously unavailable information on the origin and mechanisms of HSC generation. These data show that, while the 45-fold expansion of CFU-C progenitors can be explained by rapid proliferation (five to seven divisions over 4 days), the process of extensive CFU-S and HSC formation (230- and 150-fold increase, respectively)

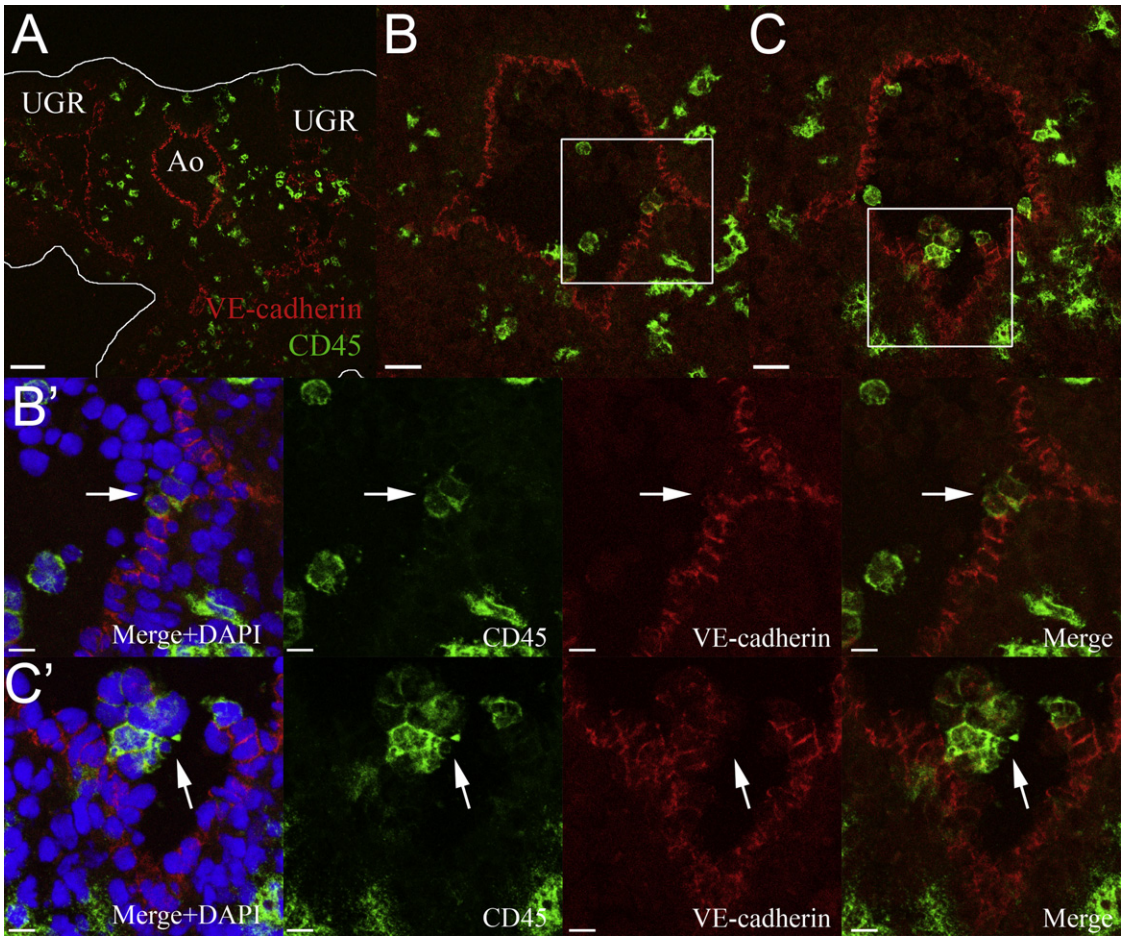

Figure 5. VE-Cadherin and CD45 Coexpressing Cells Are Specifically Associated with the Dorsal Aorta

(A) Transverse section through an E11.5 AGM region showing CD45 (green) and VE-cadherin (red) expression. The boundary of the region is outlined. Note that CD45-expressing cells are present within the urogenital ridges (UGR) and the area of the dorsal aorta (Ao) and para-aortic mesenchyme. Ventral side is orientated down (scale bar, 70 μm).

(B) Representative example of VE-cadherin$^+$CD45$^+$ cells integrated into the ventral endothelial lining of the dorsal aorta (scale bar, 30 μm).

(C) Representative example of a ventral intra-aortic hematopoietic cluster composed of VE-cadherin$^+$CD45$^+$ cells (scale bar, 30 μm).

(B′ and C′) Digital zoom of respective boxed regions in (B) and (C) providing a detailed representation of the coexpression of VE-cadherin and CD45 on indicated cells (arrow; scale bar, 11 μm). DAPI-stained nuclei are shown in blue. Images are representative of the analysis of sequential sections from three individual E11.5 AGM regions.

must occur predominantly through a maturation process. By replacing cell populations with analogous sorted EGFP-positive fractions, we demonstrated that HSC specification within the E11.5 AGM region occurs via the acquisition of stem cell functions by CD45$^+$ cells.

Previously, we and others have characterized the CD45$^+$ compartment in the E11.5 AGM region and identified two functionally distinct populations (North et al., 2002; Taoudi et al., 2005). The major population (VE-cadherin$^-$CD45$^+$) predominantly contains mature hematopoietic cells and a low frequency of progenitor cells. The second, a rare VE-cadherin$^+$CD45$^+$ population, is enriched for blast-like cells and contains a high frequency of hematopoietic progenitors. Importantly, the VE-cadherin$^+$CD45$^+$ population also harbors the single definitive HSC detectable in the E11.5 AGM region.

To determine which of these CD45$^+$ subpopulations matures into definitive HSCs, we purified them separately from the E11.5 AGM region (from EGFP embryos) and, following coreaggregation with wild-type AGM microenvironment, transplanted small doses of cultured cells into irradiated recipients. While VE-cadherin$^-$CD45$^+$ cells were not able to give rise to HSCs, the VE-cadherin$^+$CD45$^+$ fraction was highly efficient in producing definitive HSCs as all transplanted mice were reconstituted.

We found that some VE-cadherin$^+$CD45$^+$ cells have a cuboid shape and are integrated into the endothelial lining of the dorsal aorta. Rare solitary VE-cadherin$^+$CD45$^+$ cells are also found on the luminal surface of the dorsal aorta. However, the vast majority of the VE-cadherin$^+$CD45$^+$ cells in the AGM region are organized as intra-aortic clusters.

If the formation of HSCs occurs via "budding" from the endothelial lining, as has been previously speculated (Dzierzak and Speck, 2008), this may be initiated via upregulation of CD45 in emerging pre-HSCs within the endothelial layer (specification of pre-HSCs), as illustrated in Figure 7. Alternatively, the

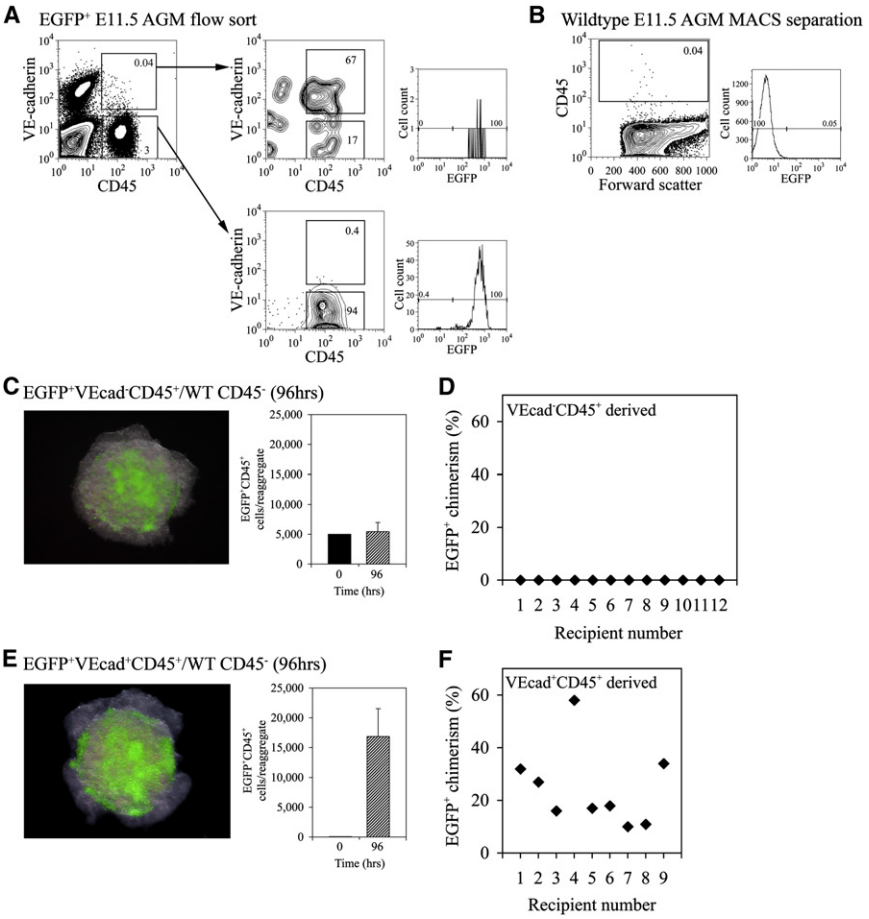

Figure 6. Pre-HSCs in the E11.5 AGM Region Are Identified by the VE-Cadherin$^+$CD45$^+$ Immunophenotype

(A) Representative example of sort criteria and purity checks used to purify VE-cadherin$^+$CD45$^+$ and VE-cadherin$^-$CD45$^+$ populations from the fresh EGFP$^+$ E11.5 AGM regions.

(B) Representative example of CD45$^-$ cells purified from fresh wild-type (WT) E11.5 AGM regions.

(C) AGM chimeric reaggregates were generated from 5,000 EGFP$^+$ VE-cadherin$^-$CD45$^+$ and 135,000 WT CD45$^-$ cells and cultured for 96 hr. Shown is an example of such a reaggregate (EGFP fluorescence/bright-field merge, original magnification 50×) and the numbers of EGFP$^+$ CD45$^+$ cells before (0 hrs) and after ex vivo development (96 hrs) (two independent experiments ± SEM).

(D) After 96 hr, a 0.05 dose of reaggregate was transplanted into each recipient mouse; 0 out of 12 were reconstituted.

(E) Chimeric reaggregates were generated from purified 70 EGFP+ VE-cadherin$^+$CD45$^+$ cells and 135,000 WT CD45$^-$ cells. Shown is an example of such a reaggregate (EGFP fluorescence/bright-field merge, original magnification 50×) and the numbers of EGFP$^+$CD45$^+$ cells before (0 hrs) and after ex vivo development (96 hrs) (two independent experiments ± SEM).

(F) Following transplantation of a 0.05 dose of reaggregate per recipient, all nine out of nine mice were reconstituted at a high level.

incorporation of an external specialized precursor, e.g., from subendothelial mesenchyme, into the endothelial layer cannot be ruled out (Bertrand et al., 2005; North et al., 2002). Further invagination of the endothelial lining results in formation of the epithelial-like buds (concomitant with formation of characteristic indentation of the endothelial lining) containing expanded VE-cadherin$^+$CD45$^+$ pre-HSCs that are not yet functional definitive HSCs. Further studies to directly investigate the source of pre-HSCs will be needed to substantiate this model.

It will be one of the key future challenges to understand the cascade of molecular events leading initially to specification of the pre-HSC and the subsequent formation of definitive HSCs. The culture system described here provides a powerful tractable resource for further analysis of cellular compartments constituting complex HSC niches and the molecular networks underlying the specification and expansion of definitive HSCs.

EXPERIMENTAL PROCEDURES

Mice

Mice were housed and bred in animal facilities at the University of Edinburgh in compliance with Home Office regulations. Embryos were generated from the pairing of either C57BL/6 or C57BL/6 aEGFP females (Gilchrist et al., 2003) with CBA or C57BL/6 stud males. The morning after discovering a vaginal plug was designated as day 0.5. The developmental stage of embryos was determined according to Theiler's criteria.

Tissue Culture

E11.5 AGM regions were dissected and dissociated as previously described (Kumaravelu et al., 2002).

Organ Explant

Whole AGM regions were cultured as previously described, except steel meshes were not used and organs were cultured in IMDM$^+$ medium (IMDM [Invitrogen], 20% fetal calf serum, L-glutamine [4 mM], penicillin/streptomycin [50 units/ml], mercaptoethanol [0.1 mM], IL-3 [100 ng/ml], SCF [100 ng/ml], and Flt3L [100 ng/ml]; growth factors were purchased from Peprotech). Tissues were maintained in 5% CO_2 at 37°C in a humidified incubator.

Submersion Culture

In 250 μl IMDM$^+$, one equivalent of dissociated AGM cells was cultured in U- or V-bottom 96-well tissue culture plates (Bibby Sterilin).

Reaggregation Technique

Dissociated cells were resuspended in 10 μl of IMDM$^+$ per one AGM equivalent. Reaggregates (one embryo equivalent per reaggregate) were made by centrifugation in a yellow tip occluded by parafilm at 300 × g for 5 min and cultured on the top of a 0.65 μm Durapore filter (Millipore, Cat. No. DVPP02500) at the gas-liquid interface. This technique in application to the thymus is described in J.S. et al., unpublished data.

CFU-C Assay

Colony development was performed using M3434 medium (StemCell Technologies) according to the manufacturer's instructions. Colonies were scored after 7–9 days.

Long-Term Repopulation Assay

Donor tissues from Ly5.2/2 embryos were isolated, cultured, and transplanted into irradiated Ly5.2/1 adult recipients as described previously (Kumaravelu

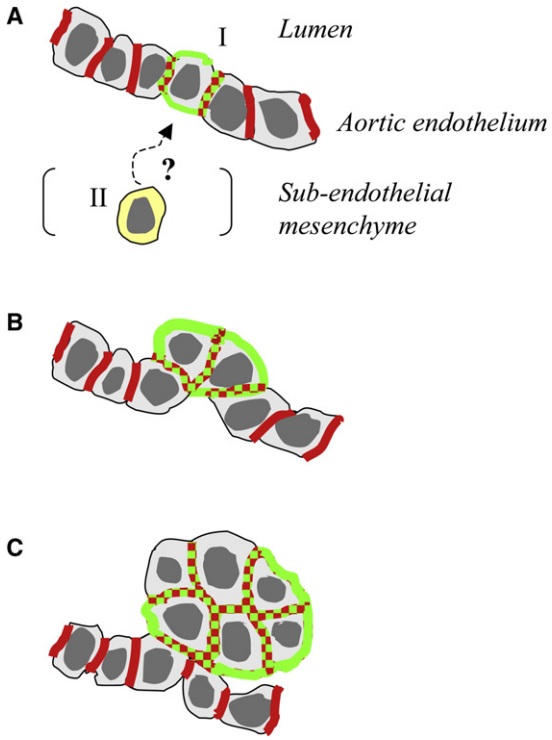

Figure 7. Proposed Model for the Development of Pre-HSCs within Intra-Aortic Clusters

(A) Specification of a VE-cadherin$^+$CD45$^+$ (double-positive, DP) cell by upregulation of CD45 in the endothelial lining (scenario I). It cannot be ruled out that, alternatively, an external precursor (e.g., from subendothelial mesenchyme) integrates into the endothelial lining (scenario II).

(B) Initiation of the invagination of the endothelial layer led by DP cells (hematopoietic by nature) is accompanied by formation of a characteristic indentation of the lining (also see Figure 5).

(C) Formation of the epithelial-like "bud" formed mainly by the DP population enriched for pre-HSCs. The vast majority of DP cells in E11.5 AGM region are organized in clusters (two to four clusters per E11.5 AGM region). Red, localization of VE-cadherin; green, localization of CD45. Colocalization of VE-cadherin and CD45 is indicated by red-green dotted line.

et al., 2002). The number of transplanted cultured cells is expressed throughout the article in doses and defined as a unit of cells equivalent to their number present in one cultured organ; for example, a 0.05 dose is equal to 5% of the cells present in one cultured organ. Donor cells were coinjected with 20,000 Ly5.1/1 bone marrow cells. Donor chimerism was determined as described previously (Taoudi and Medvinsky, 2007).

Phenotypic Identification of HSCs

Cellular suspensions were stained with the appropriate combination using the following monoclonal antibodies: anti-CD45, anti-PECAM-1, anti-Sca1, anti-cKit, and anti-CD34. Donor contribution was assessed by flow cytometry using anti-Ly5.2-PE and anti-Ly5.1-APC antibodies (BD Biosciences). Mice demonstrating $\geq$5% donor-derived chimerism (contributing to both myeloid and lymphoid lineages) after a minimum of 16 weeks were considered to be reconstituted. Limiting dilution analysis was performed using L-Calc software (Stem Cell Technologies).

CFU-S Assay

Cells were transplanted into irradiated adult mice. After 11 days, recipient spleens were dissected, fixed in Bouin's solution, and macroscopic colonies counted. When using EGFP$^+$ donor tissues, spleens were directly examined without fixation. Images were captured using a MZFLIII dissecting microscope (Leica).

Cell Cycle Analysis

Cell cycle analysis was performed using the BrdU Flow Kit (BD Bioscience). In brief, reaggregates were removed from filters and submersed in IMDM$^+$ medium containing 10 μM BrdU for 30 min at 37°C. Reaggregates were then washed and dissociated. After staining with anti-CD45 and anti-PECAM-1 antibodies, cells were fixed and processed according to the manufacturer's instructions. Dead cells and debris were excluded on the basis of scatter profile. Data were acquired using a FACScalibur (BD Biosciences) and analyzed using FlowJo software (TreeStar).

Carboxyfluorescein Diacetate Succinimidyl Ester Pulse/Chase

CFSE (Invitrogen) was stored as a 5 mM solution in DMSO at −20°C. Cellular suspension from E11.5 AGM was loaded with CFSE as follows: cells from the E11.5 AGM region (1 × 10^6 cells per ml) were incubated in 10 μM CFSE, diluted in 7% FCS/PBS ($Mg^{2+}Ca^{2+}$ free) for 10 min at 37°C. Reaction volume was made up to 5.0 ml with ice-cold 10% FSC/PBS ($Mg^{2+}Ca^{2+}$ free) and incubated on ice for 5 min. Cells were centrifuged for 5 min at 300 × g, resuspended in 1.0 ml, and recentrifuged. Reaggregates were produced and maintained as described above. Dead cells and debris were excluded on the basis of scatter profile. CFSE content in viable cells was detected using a FACScalibur.

Cytological Examination

Following purification, cells were processed as previously described (Taoudi et al., 2005).

Confocal Microscopy

Tissues were embedded in O.C.T. by flash-freezing samples on dry ice. 10 μM sections were produced using a CM1900 cryostat (Leica). Three-dimensional reconstructions were processed as previously described (Taoudi and Medvinsky, 2007). Images were captured using an upright confocal microscope (DM IRE2, Leica) and processed using Abode Photoshop CS2. The following antibodies were used: anti-VE-cadherin-Alexa647, anti-CD45-APC/biotin/purified, anti-PECAM-1-PE, and anti-Sca1-PE. Either anti-rat Alexa488 or Alexa647 conjugated streptavidin (Molecular Probes, Invitrogen) was used to detect primary antibodies. Antibodies were purchased from either BD Biosciences or eBioscience.

Lineage-Tracing Experiments

AGM regions were dissected from either wild-type or EGFP mouse lines and cellular suspensions produced. Cell suspensions were stained with anti-CD45-biotin antibodies for 20 min in the dark on ice. Cells were then labeled within streptavidin-conjugated magnetic beads (MiltenyiBiotec); CD45$^+$ and CD45$^-$ fractions were separated by MACS (MiltenyiBiotec) according to manufacturer's instructions. Purity checks were performed on aliquots from the collected samples following restaining with streptavidin-conjugated APC and anti-CD45-APC. Approximately one equivalent of E11.5 AGM cells was reaggregated and cultured. For VE-cadherin/CD45 lineage-tracing experiments, cells from EGFP embryos were purified by flow cytometry (MoFlo, DacoCytomation), as previously described (Taoudi et al., 2005), and then reaggregated with MACS-purified WT CD45$^-$ cells. Experiments were set up in either duplicate or triplicate.

SUPPLEMENTAL DATA

Supplemental Data for this article, including Supplemental Figures, can be found online at http://www.cellstemcell.com/cgi/content/full/3/1/99/DC1/.

ACKNOWLEDGMENTS

We thank Carol Manson, John Verth, and Yvonne Gibson for animal maintenance and recipient irradiation; Jan Vrana for cell sorting. We thank David Hills, Tilo Kunath, Sally Lowell, and Val Wilson for useful comments on the manuscript. This research was supported by funding from the Leukaemia Research Fund, Biotechnology and Biological Sciences Research Council, Medical Research Council, the Mabel Green endowment, and the EU FPVI integrated project EuroStemCell.

Received: February 13, 2008
Revised: April 23, 2008
Accepted: June 9, 2008
Published: July 2, 2008

REFERENCES

Anderson, G., Jenkinson, E.J., Moore, N.C., and Owen, J.J. (1993). MHC class II-positive epithelium and mesenchyme cells are both required for T-cell development in the thymus. Nature *362*, 70–73.

Baumann, C.I., Bailey, A.S., Li, W., Ferkowicz, M.J., Yoder, M.C., and Fleming, W.H. (2004). PECAM-1 is expressed on hematopoietic stem cells throughout ontogeny and identifies a population of erythroid progenitors. Blood *104*, 1010–1016.

Bertrand, J.Y., Giroux, S., Golub, R., Klaine, M., Jalil, A., Boucontet, L., Godin, I., and Cumano, A. (2005). Characterization of purified intraembryonic hematopoietic stem cells as a tool to define their site of origin. Proc. Natl. Acad. Sci. USA *102*, 134–139.

Cumano, A., Ferraz, J.C., Klaine, M., Di Santo, J.P., and Godin, I. (2001). Intraembryonic, but not yolk sac hematopoietic precursors, isolated before circulation, provide long-term multilineage reconstitution. Immunity *15*, 477–485.

de Bruijn, M.F., Speck, N.A., Peeters, M.C., and Dzierzak, E. (2000). Definitive hematopoietic stem cells first develop within the major arterial regions of the mouse embryo. EMBO J. *19*, 2465–2474.

Dzierzak, E., and Medvinsky, A. (1995). Mouse embryonic hematopoiesis. Trends Genet. *11*, 359–366.

Dzierzak, E., and Speck, N.A. (2008). Of lineage and legacy: the development of mammalian hematopoietic stem cells. Nat. Immunol. *9*, 129–136.

Ferkowicz, M.J., Starr, M., Xie, X., Li, W., Johnson, S.A., Shelley, W.C., Morrison, P.R., and Yoder, M.C. (2003). CD41 expression defines the onset of primitive and definitive hematopoiesis in the murine embryo. Development *130*, 4393–4403.

Gekas, C., Dieterlen-Lievre, F., Orkin, S.H., and Mikkola, H.K. (2005). The placenta is a niche for hematopoietic stem cells. Dev. Cell *8*, 365–375.

Gilchrist, D.S., Ure, J., Hook, L., and Medvinsky, A. (2003). Labeling of hematopoietic stem and progenitor cells in novel activatable EGFP reporter mice. Genesis *36*, 168–176.

Grobstein, C. (1953). Inductive epitheliomesenchymal interaction in cultured organ rudiments of the mouse. Science *118*, 52–55.

Kumaravelu, P., Hook, L., Morrison, A.M., Ure, J., Zhao, S., Zuyev, S., Ansell, J., and Medvinsky, A. (2002). Quantitative developmental anatomy of definitive haematopoietic stem cells/long-term repopulating units (HSC/RUs): role of the aorta-gonad-mesonephros (AGM) region and the yolk sac in colonisation of the mouse embryonic liver. Development *129*, 4891–4899.

Lyons, A.B. (1999). Divided we stand: tracking cell proliferation with carboxyfluorescein diacetate succinimidyl ester. Immunol. Cell Biol. *77*, 509–515.

Matsuoka, S., Ebihara, Y., Xu, M., Ishii, T., Sugiyama, D., Yoshino, H., Ueda, T., Manabe, A., Tanaka, R., Ikeda, Y., et al. (2001). CD34 expression on long-term repopulating hematopoietic stem cells changes during developmental stages. Blood *97*, 419–425.

Medvinsky, A., and Dzierzak, E. (1996). Definitive hematopoiesis is autonomously initiated by the AGM region. Cell *86*, 897–906.

Morrison, S.J., Hemmati, H.D., Wandycz, A.M., and Weissman, I.L. (1995). The purification and characterization of fetal liver hematopoietic stem cells. Proc. Natl. Acad. Sci. USA *92*, 10302–10306.

Moscona, A., and Moscona, H. (1952a). The dissociation and aggregation of cells from organ rudiments of the early chick embryo. J. Anat. *86*, 287–301.

Moscona, H., and Moscona, A. (1952b). The development in vitro of the anterior lobe of the embryonic chick pituitary. J. Anat. *86*, 278–286.

North, T.E., de Bruijn, M.F., Stacy, T., Talebian, L., Lind, E., Robin, C., Binder, M., Dzierzak, E., and Speck, N.A. (2002). Runx1 expression marks long-term repopulating hematopoietic stem cells in the midgestation mouse embryo. Immunity *16*, 661–672.

Ohneda, O., Fennie, C., Zheng, Z., Donahue, C., La, H., Villacorta, R., Cairns, B., and Lasky, L.A. (1998). Hematopoietic stem cell maintenance and differentiation are supported by embryonic aorta-gonad-mesonephros region-derived endothelium. Blood *92*, 908–919.

Oostendorp, R.A., Harvey, K.N., Kusadasi, N., de Bruijn, M.F., Saris, C., Ploemacher, R.E., Medvinsky, A.L., and Dzierzak, E.A. (2002). Stromal cell lines from mouse aorta-gonads-mesonephros subregions are potent supporters of hematopoietic stem cell activity. Blood *99*, 1183–1189.

Osawa, M., Hanada, K., Hamada, H., and Nakauchi, H. (1996). Long-term lymphohematopoietic reconstitution by a single CD34-low/negative hematopoietic stem cell. Science *273*, 242–245.

Ottersbach, K., and Dzierzak, E. (2005). The murine placenta contains hematopoietic stem cells within the vascular labyrinth region. Dev. Cell *8*, 377–387.

Robin, C., Ottersbach, K., Durand, C., Peeters, M., Vanes, L., Tybulewicz, V., and Dzierzak, E. (2006). An unexpected role for IL-3 in the embryonic development of hematopoietic stem cells. Dev. Cell *11*, 171–180.

Shannon, J.M., and Hyatt, B.A. (2004). Epithelial-mesenchymal interactions in the developing lung. Annu. Rev. Physiol. *66*, 625–645.

Taoudi, S., and Medvinsky, A. (2007). Functional identification of the hematopoietic stem cell niche in the ventral domain of the embryonic dorsal aorta. Proc. Natl. Acad. Sci. USA *104*, 9399–9403.

Taoudi, S., Morrison, A.M., Inoue, H., Gribi, R., Ure, J., and Medvinsky, A. (2005). Progressive divergence of definitive haematopoietic stem cells from the endothelial compartment does not depend on contact with the foetal liver. Development *132*, 4179–4191.

Townes, P., and Holtfreter, J. (1955). Directed movements and selective adhesion of embryonic amphibian cells. J. Exp. Zool. *128*, 53–120.

Uchida, N., and Weissman, I.L. (1992). Searching for hematopoietic stem cells: evidence that Thy-1.1lo Lin- Sca-1+ cells are the only stem cells in C57BL/Ka-Thy-1.1 bone marrow. J. Exp. Med. *175*, 175–184.

White, A., Carragher, D., Parnell, S., Msaki, A., Perkins, N., Lane, P., Jenkinson, E., Anderson, G., and Caamano, J.H. (2007). Lymphotoxin a-dependent and -independent signals regulate stromal organizer cell homeostasis during lymph node organogenesis. Blood *110*, 1950–1959.

Xu, M.J., Tsuji, K., Ueda, T., Mukouyama, Y.S., Hara, T., Yang, F.C., Ebihara, Y., Matsuoka, S., Manabe, A., Kikuchi, A., et al. (1998). Stimulation of mouse and human primitive hematopoiesis by murine embryonic aorta-gonad-mesonephros-derived stromal cell lines. Blood *92*, 2032–2040.